# Statistics of lateral atom manipulation by atomic force microscopy at room temperature

Yoshiaki Sugimoto,[1,*] Koutaro Miki,[1] Masayuki Abe,[1,2] and Seizo Morita[1]
[1]*Graduate School of Engineering, Osaka University, 2-1 Yamada-Oka, Suita, Osaka 565-0871, Japan*
[2]*PRESTO, Japan Science and Technology Agency Kawaguchi, Saitama 332-0012, Japan*
(Received 29 August 2008; published 4 November 2008)

We perform vacancy-mediated lateral manipulations of Si adatoms on the Si(111)-(7×7) surface by atomic force microscopy at room temperature. A variety of line profiles associated with different atom hopping processes is observed in successive topographic line scans for the atom manipulations. Atom manipulation statistics show stochastic behavior in atom movements. The probability of atom movement increases with a decrease in the tip-surface distance. Moreover, it depends on the scan direction, even with crystallographic equivalence, because of tip apex asymmetry. In addition, the hopping rate reflects the difference in stability of the adsorption sites of the manipulated atoms.

DOI: 10.1103/PhysRevB.78.205305 PACS number(s): 68.37.Ps, 68.35.bg, 68.47.Fg

Since the sophisticated atom manipulation experiment reported by Eigler,[1] single atom manipulation and assembly by scanning tunneling microscopy (STM) has attracted much attention because of the intriguing applications in nanofabrication and nanoscience.[2–4] In recent years, we have developed an atom manipulation technique using noncontact atomic force microscopy (NC-AFM), which has proven to be a powerful tool for imaging individual atoms on insulating as well as conducting surfaces,[5] force spectroscopic measurements between single atoms,[6] and even chemical identification.[7] After the first demonstration of the vertical[8] and lateral[9] manipulations of single atoms using NC-AFM at low temperature, we have achieved well-controlled atom manipulation and assembly even at room temperature.[10] Furthermore, the mechanism of room-temperature lateral manipulation of single Si adatoms on the Si(111)-(7×7) surface by NC-AFM was investigated using a combination of experiments and first-principles calculations.[11] This study has elucidated that a Si adatom is manipulated by a local reduction in the natural diffusion barrier below the limit that enables thermally activated hopping to adjacent adsorption sites by the attractive chemical bonding force between the tip and the adatom. The stochastic behavior expected in thermally activated lateral atom manipulation has also been investigated by simulations on the MgO(100) surface.[12–14] However, as far as we know, quantitative NC-AFM experiments indicating the stochastic behavior in lateral atom manipulation has not been reported yet.

In the present study, we investigate the stochastic behavior of atom hopping on the Si(111)-(7×7) surface by NC-AFM at room temperature. Various line profiles associated with different atom hopping processes are obtained in successive line scans during the manipulation. The atom manipulation statistics show that the atom hopping rate depends on the tip-surface distance, the asymmetry of the tip apex, and the adsorption sites.

The experiment was performed using a home-built NC-AFM apparatus with the frequency modulation technique[5,15] at room temperature. The deflection of commercial cantilevers was detected using a home-built interferometer. The frequency shift ($\Delta f$) from the resonance frequency of the cantilever oscillated at constant amplitude was detected using a phase-locked-loop-based AFM controller and frequency demodulator (easyPLL plus detector and controller, Nanosurf, Liestal, Switzerland). NC-AFM topographic imaging and single atom manipulation were performed using a commercial digital scanning probe microscope controller (Dulcinea, Nanotec, S. L., Madrid, Spain).[16] Because the sharp and clean Si tip apex was prepared by Ar ion sputtering, we can routinely obtain atomic resolution images from the first scanning after preparation. The Si(111)-(7×7) reconstructed surfaces were prepared by the standard method of flashing and annealing the samples. The contact potential difference was compensated by applying a bias voltage to the sample with respect to the grounded tip.

In this paper, natural Si adatoms were manipulated along the $[1\bar{1}0]$ direction using a vacancy site as an open space, which is an essential part of this lateral atom manipulation, as we have reported before.[11] These atomic vacancies can be created by the artificial atom extraction[8] or are occasionally found. Statistics of atom manipulation were acquired as follows. First, using an atom-tracking technique,[17,18] the tip was precisely positioned on top of a Si adatom. This Si adatom was selected such that the scanning line for atom manipulation corresponded to the line connecting the vacancy and the Si adatom. In the schematic view of Fig. 1(a), the locations of the Si adatom and the vacancy are illustrated as a solid circle indicated by the arrow and dotted circle, respectively. After measurement of the drift velocity, we compensated for thermal drift by applying voltage to the corresponding electrodes of the piezoelectric scanner using a feedforward controller.[19,20] Then, we performed successive topographic line scans along the path connecting the Si adatom used for tip positioning and the vacancy, as shown by the arrow in Fig. 1(a). These line scans were performed by lifting the tip up, typically 1 Å above the surface on the way back. Finally, the tip-surface distance was gradually decreased by increasing the $|\Delta f|$ set point for feedback until successive atom hopping events were observed.

Images (i), (ii), and (iii) in Fig. 1(a) indicate typical NC-AFM topographies of successive line scans above the adatoms in the unfaulted half-unit cells with the passage of time. The fast scan direction is from left to right for (i) and (iii) and is reversed for (ii). The tip-surface interaction is increased in (iii) compared with (i) and (ii) by decreasing the

 

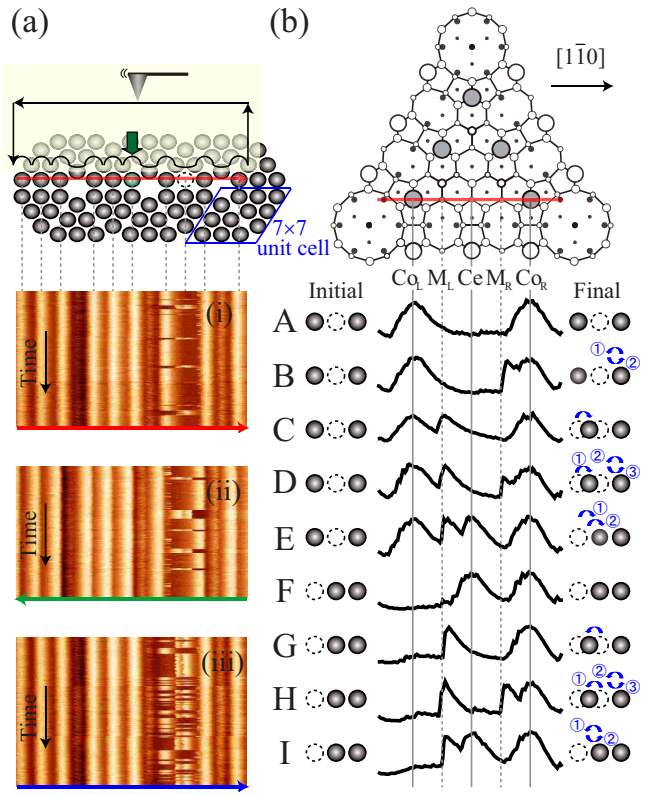


FIG. 1. (Color online) Statistical experiments of lateral atom manipulation on the Si(111)-(7×7) surface. (a) NC-AFM topographic images of successive line scans above the same line on the Si(111)-(7×7) surface with the passage of time, which were obtained as shown in the schematic view in the top panel. The acquisition parameters including the resonance frequency, cantilever oscillation amplitude, spring constant, and $Q$ factor are $f_0$=152 337.1 Hz, $A$=144 Å, $k$=24.4 N/m, and $Q$=9600, respectively. [(i) and (ii)] $\Delta f$=−6.4 Hz and (iii) $\Delta f$=−7.0 Hz. The fast scan velocity is 8.7 nm/s. The fast scan direction of (ii) is opposite to those of (i) and (iii). (b) The nine different types of line profiles with schematic views of the initial and final configurations of adatoms and atom hopping steps. Each adsorption site is illustrated in the model of the Si(111)-(7×7) surface in the top panel.

tip-surface distance. We observed that successive line scans induce the movement of the vacancy position: Si adatoms are laterally manipulated among the adsorption sites. The adsorption sites, such as corner adatoms (Co$_L$ and Co$_R$), a center adatom (Ce), and metastable sites (M$_L$ and M$_R$), are illustrated in the schematic model of the Si(111)-(7×7) surface in the top panel of Fig. 1(b), which has a vacancy on the Ce site. In the M$_L$ and M$_R$ sites, the adatom sits in a $T_4$ configuration bonded to one of the three original surface rest atoms.[11]

The topographic images in Fig. 1(a) include nine different types of line profiles associated with various atom hopping behaviors, as shown in Fig. 1(b). Initial and final atom configurations and atom hopping steps are illustrated near each line profile. Solid circles and dotted circles represent adatoms and vacancies, respectively, and arrows indicate the atom hopping steps. In type A–E of line profiles, a vacancy is initially located at the Ce site, while in F to I, it is at the Co$_L$ site. Each type of line profile is explained as follows. In type A, two adatoms are imaged at the Co$_L$ and Co$_R$ sites, and the vacancy is at the Ce site. In this case, no signature of atom movement is observed. In type B, once the adatom at Co$_L$ site and the vacancy have been imaged, the feedback mechanism suddenly retracts the tip at the M$_R$ position due to the jump of the right corner adatom toward the tip. Then, while imaging the adatom at the M$_R$ site, the adatom jumps back to the Co$_R$ site where the adatom is imaged again. In types C and D, the tip initially encounters and passes over the adatom at the Co$_L$ site and is suddenly retracted due to the jump of the adatom from the Co$_L$ to the M$_L$ site, where it stays without further movement. An adatom at the Co$_R$ site is just imaged in type C, while the adatom at the Co$_R$ site moves to the M$_R$ site and jumps back to the Co$_R$ site in type D, as in type B. In type E, the tip initially encounters and passes over the adatom at the Co$_L$ site and is suddenly retracted due to the jump of the adatom from the Co$_L$ site to the M$_L$ site, from which it subsequently jumps again to the Ce site. Finally, the adatom is imaged at the center site, together with the one at the Co$_R$ site that does not move. In type F, two adatoms are imaged at the Ce and Co$_R$ sites and the vacancy is at the Co$_L$ site. In this case, no signature of atom movement is observed. In types G and H, just after the vacancy is imaged, the center adatom jumps toward the tip and adsorbs at the M$_L$ site where it stays without further movement. The adatom at the Co$_R$ site is just imaged in type G, while the adatom at the Co$_R$ site moves to the M$_R$ site and jumps back to the Co$_R$ site in type H, as in types of B and D. In type I, after the vacancy is imaged, the center adatom jumps toward the tip and adsorbs at the M$_L$ site; it returns to the Ce site afterward. Although the line profiles of types C, D, G, and H show that the adatom temporarily stays at the M$_L$ site, these adatoms were observed at the Co$_L$ site as initial positions in the next line scans. Therefore, the adatom that adsorbs at the M$_L$ site thermally hops to the Co$_L$ site with no short-range tip-surface interaction. In contrast, we have never observed thermal hopping from the M$_L$ site to the Ce site because of the difference in adsorption energy, as we will discuss below.

In all the atom hopping observed here, adatoms move toward the tip. This indicates that attractive interaction forces with the tip apex pull the adatoms. This lateral atom manipulation can be classified into the so-called pulling mode, which has been proposed in lateral manipulation experiments by low-temperature STM.[2] Our experimental results indicate that under the same initial atom configurations, different atom hopping processes were observed by tip scanning with the same parameters. Five (four) different profiles were obtained even under the same initial conditions of A–E (F–I). This stochastic behavior observed in lateral atom manipulation is consistent with the thermally assisted hopping mechanism that we have applied to explain atom manipulation of the same system.[11]

To provide further insights into the stochastic behavior of atom movements, we calculated the hopping rates of successful movements. Figure 2 shows the probabilities, expressed as percentages, with illustrations of the initial and final atom configurations and the tip trajectory. The analysis is based on a total of 2131 line profiles obtained in the same session as the experiments in Fig. 1. For example, Fig. 2(a)

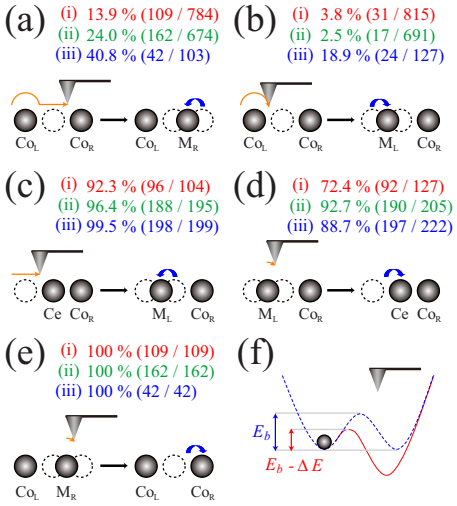


FIG. 2. (Color online) [(a)–(e)] The probabilities of atom movement for five different atom hopping steps. The initial and final atom configurations and scanning tip trajectory are illustrated. Setting $n(X)$ as the number of the observed line profiles of type $X$, where $X$ is from A to I in Fig. 1(b), the probabilities are calculated by (a) $n(\mathrm{B})/[n(\mathrm{A})+n(\mathrm{B})]$, (b) $[n(\mathrm{C})+n(\mathrm{D})+n(\mathrm{E})]/[n(\mathrm{A})+n(\mathrm{B})+n(\mathrm{C})+n(\mathrm{D})+n(\mathrm{E})]$, (c) $[n(\mathrm{G})+n(\mathrm{H})+n(\mathrm{I})]/[n(\mathrm{F})+n(\mathrm{G})+n(\mathrm{H})+n(\mathrm{I})]$, (d) $[n(\mathrm{E})+n(\mathrm{I})]/[n(\mathrm{C})+n(\mathrm{D})+n(\mathrm{E})+n(\mathrm{G})+n(\mathrm{H})+n(\mathrm{I})]$, and (e) $n(\mathrm{B})/n(\mathrm{B})$. The probabilities of (i), (ii), and (iii) correspond to the scan conditions of Fig. 1 (i), (ii), and (iii), respectively. (f) The schematic model of the potential landscape for thermally activated atom manipulation. The solid (dashed) curve is the potential landscape with (without) tip-surface interaction. The tip-adatom interaction reduces the energy barrier ($E_b$) in the surface potential landscape by $\Delta E$.

shows the probability of successful atom movement from the $\mathrm{Co}_R$ site to the $\mathrm{M}_R$ site when the tip passes over $\mathrm{M}_R$ site. Since the number of profiles of type B (type A) in Fig. 1(b) is the number of successful (unsuccessful) atom manipulations, the probability can be calculated using the number of type B profiles divided by the sum of the number of type A and B profiles. In the same way, other probabilities were calculated as described in the caption of Fig. 2. The probabilities of conditions (i), (ii), and (iii) in Fig. 2 correspond to the scan conditions of images (i), (ii), and (iii) in Fig. 1(a), respectively. The scan direction of (ii) is opposite to that of (i) and (iii). To discuss dependence of the probability on the scan direction with respect to the orientation of the asymmetric tip, images under the same scan condition as (ii) were analyzed after the images were reversed horizontally. The line scans from left to right and from right to left are equivalent because of the surface symmetry if the tip is not taken into account. The only difference between (i) and (ii) is the orientation of the tip apex with respect to the scan direction.

From the atom hopping probability, we can estimate the energy barrier reduced by the tip-surface interaction, $E_b-\Delta E$ [see Fig. 2(f)]. The rate of thermally activated atom hopping is described by the Arrhenius formula, $\nu=\nu_0 \exp(-\frac{E_b-\Delta E}{k_B T})$, where $\nu_0$ and $k_B T$ are the prefactor and thermal energy, respectively. We can estimate $E_b-\Delta E$ under condition (i) of Fig. 2(b) as follows. The tip scanning took 1 s per one line, and the topographic data for 512 pixels were acquired in each line scan. Since atom hopping occurs at almost the same lateral tip position within an error range of about 1 pixel, the residence time of the lateral tip position, where atom manipulation can occur, can be estimated as 1/512 s. In addition, since the tip is oscillated at large amplitude in this study, manipulation can occur in short periods when the tip is sufficiently close to the surface to reduce the diffusion barrier for manipulation. Assuming that the energy barrier can be sufficiently reduced by tip locations within a range of 0.1 Å from the closest point to the surface in the entire vertical tip motion of 288 Å, the duration of time for the manipulation can be estimated to be 1.2% of the total time. Therefore, the tip has 1.2% of 1/512 s per each line scan to reduce the energy barrier for atom manipulation. Since atom hopping from $\mathrm{Co}_L$ to $\mathrm{M}_L$ site was observed in 31 line scans out of a total of 815 under condition (i) of Fig. 2(b), we obtain $\nu=1.6\times10^3$ Hz. Setting $\nu_0=1\times10^{13}$ Hz, a typical value on semiconductor surfaces[21] and $T=300$ K, we obtain $E_b-\Delta E=584$ meV. Despite the roughness of the estimation, this value is in good agreement with 650 meV, the dominant energy barrier for the transition from $\mathrm{Co}_L$ to $\mathrm{M}_L$ site that was theoretically obtained assuming a tip-surface distance of 3.5 Å.[11] Nevertheless, the absolute tip-surface distance, which cannot be obtained from the experiment, and the strength of the interaction force as well as the tip apex structure may be different between theory and the present experiment.

Figure 2 clearly shows that a decrease in tip-to-surface distance increases the atom hopping rate: the hopping rate at a small tip-surface distance (iii) is larger than that at a greater tip-surface distance (i) for all atom hopping cases. For example, the probability of atom hopping from $\mathrm{Co}_L$ to $\mathrm{M}_L$ site [3.8% for (i)] in Fig. 2(b), which is an important step for atom manipulation from $\mathrm{Co}_L$ to Ce site,[11] is drastically increased to 18.9% for (iii) with a decrease in the tip-surface distance. This increase in the hopping rate should be attributed to enhancement of the tip-adatom attractive interaction, which reduces the diffusion barrier for thermally activated atom hopping. We can estimate the difference in the reduction in the energy barrier between the two tip-surface distances. For example, in Fig. 2(b) this difference can be estimated to be 42 meV from the ratio between the probabilities of (i) and (iii), with no assumption about the value of $\nu_0$.

Moreover, comparing the atom hopping rates of (i) and (ii) reveals that the rates depend strongly on the orientation of the tip apex with respect to the scan direction. For instance, in Fig. 2(a), the probability of successful atom movement from $\mathrm{Co}_R$ to $\mathrm{M}_R$ site in (ii) is 1.7 times larger than that in (i) for the same experimental conditions except for the orientation of the tip apex. This anisotropic hopping rate in lateral atom manipulation should be attributed to the asymmetry of the tip apex structure as theoretically predicted.[22] An atom at the very end of the tip apex forms chemical bonds with backbond atoms in the tip apex leaving a dangling bond pointing out of the apex atom toward the surface.[23] This dangling bond, from which the chemical bonding force originates, can have an anisotropy that reflects the configuration of backbond atoms.[24] In addition, the tip apex structure also influences the direction of easy relaxation of tip apex atoms under the tip-surface interaction. These

anisotropic chemical bonding forces and the anisotropy of the relaxation of the tip apex atoms lead to the anisotropy of hopping rates in lateral atom manipulation. This experimental result shows that the tip apex structure essentially affects directionality in mechanical lateral atom manipulation. We will discuss the anisotropy of the chemical bonding force arising from the tip apex structure in force maps elsewhere.[25]

By statistical atom manipulation experiments, we can also investigate the stability of the adsorption sites of the manipulated atoms. The probability of atom hopping from Ce to $M_L$ site in Fig. 2(c) is higher than that from $Co_R$ to $M_R$ site in Fig. 2(a) under all scan conditions. Because the tip scans over the vacancy and the tip-surface distance is almost the same, adatom movement is more probable from the Ce site than from the $Co_R$ site. On the other hand, the probability of atom hopping from $M_R$ to $Co_R$ site in Fig. 2(e) is higher than that from $M_L$ to Ce site in Fig. 2(d) under all scan conditions. Therefore, adatom movement to the $Co_R$ site is more probable than to the Ce site. Since this tendency was observed even using different tips, we conclude that it is preferable for a Si adatom to locate at a corner adatom site because the binding energy of a Si adatom is larger at the corner adatom site than at the center adatom site. This explanation is supported by previous STM experiments of adatom extraction[26] and displacement[27] by a voltage pulse on Si(111)-(7×7) surfaces. The extraction experiments showed that the Si adatoms at the center adatom sites are more frequently removed than those at the corner adatom sites. In the adatom displacement experiments, the center adatoms of defect-free 7×7 unit cells were laterally displaced by the voltage pulse, while displacement of corner adatoms has never been observed due to their higher binding energy.

In summary, we have reported statistical experiments on the lateral manipulation of single Si adatoms on the Si(111)-(7×7) surface by NC-AFM at room temperature. Line profiles of the NC-AFM topographic images of successive line scans show stochastic behavior of atom movements, which is consistent with thermally activated atom movement. The atom hopping rate increases with a decrease in the tip-surface distance and depends on the scan direction with respect to the orientation of the asymmetric tip. Furthermore, we found that the atom hopping rate depends on the adsorption sites of the manipulated adatoms. Understanding thermally assisted lateral atom manipulation is expected to lead to the investigation of the stability of adsorption sites and to bring us to realization of an atom-by-atom construction of nanodevices at room temperature.

The authors are grateful to A. Yurtsever for revision of the paper. This work was supported by The Grant-in-Aid for Scientific Research (Grants No. 19053006, No. 17101003, No. 18860046, and No. 19360017) from the Ministry of Education, Culture, Sports, Science, and Technology of Japan (MEXT), Japan Science and Technology Agency (JST), Handai FRC, the project Atomic Technology funded by MEXT, and 21th Century COE and Global COE programs. The work of Y.S. was supported by The Frontier Research Base for Global Young Researchers, Osaka University, on the Program of Promotion of Environmental Improvement to Enhance Young Researchers' Independence under the Special Coordination Funds for Promoting Science and Technology of MEXT.

*ysugimoto@afm.eei.eng.osaka-u.ac.jp

[1] D. Eigler and E. Schweizer, Nature (London) **344**, 524 (1990).
[2] L. Bartels, G. Meyer, and K.-H. Rieder, Phys. Rev. Lett. **79**, 697 (1997).
[3] M. Crommie, C. Lutz, and D. Eigler, Science **262**, 218 (1993).
[4] A. Heinrich, C. Lutz, J. Gupta, and D. Eigler, Science **298**, 1381 (2002).
[5] *Noncontact Atomic Force Microscopy*, edited by S. Morita, R. Wiesendanger, and E. Meyer (Springer-Verlag, Berlin, 2002).
[6] M. A. Lantz, H. J. Hug, R. Hoffmann, P. J. A. van Schendel, P. Kappenberger, S. Martin, A. Baratoff, and H. J. Guntherodt, Science **291**, 2580 (2001).
[7] Y. Sugimoto, P. Pou, M. Abe, P. Jelinek, R. Perez, S. Morita, and O. Custance, Nature (London) **446**, 64 (2007).
[8] N. Oyabu, O. Custance, I. Yi, Y. Sugawara, and S. Morita, Phys. Rev. Lett. **90**, 176102 (2003).
[9] N. Oyabu, Y. Sugimoto, M. Abe, O. Custance, and S. Morita, Nanotechnology **16**, S112 (2005).
[10] Y. Sugimoto, M. Abe, S. Hirayama, N. Oyabu, O. Custance, and S. Morita, Nature Mater. **4**, 156 (2005).
[11] Y. Sugimoto, P. Jelinek, P. Pou, M. Abe, S. Morita, R. Perez, and O. Custance, Phys. Rev. Lett. **98**, 106104 (2007).
[12] M. B. Watkins and A. L. Shluger, Phys. Rev. B **73**, 245435 (2006).
[13] T. Trevethan, M. Watkins, L. Kantorovich, A. Shluger, J. Polesel-Maris, and S. Gauthier, Nanotechnology **17**, 5866 (2006).
[14] T. Trevethan, M. Watkins, L. N. Kantorovich, and A. L. Shluger, Phys. Rev. Lett. **98**, 028101 (2007).
[15] T. R. Albrecht, P. Grütter, D. Horne, and D. Rugar, J. Appl. Phys. **69**, 668 (1991).
[16] I. Horcas, R. Fernandez, J. Gomez-Rodriguez, J. Colchero, J. Gomez-Herrero, and A. Baro, Rev. Sci. Instrum. **78**, 013705 (2007).
[17] M. Abe, Y. Sugimoto, O. Custance, and S. Morita, Appl. Phys. Lett. **87**, 173503 (2005).
[18] M. Abe, Y. Sugimoto, O. Custance, and S. Morita, Nanotechnology **16**, 3029 (2005).
[19] M. Abe, Y. Sugimoto, T. Namikawa, K. Morita, N. Oyabu, and S. Morita, Appl. Phys. Lett. **90**, 203103 (2007).
[20] Y. Sugimoto, T. Namikawa, K. Miki, M. Abe, and S. Morita, Phys. Rev. B **77**, 195424 (2008).
[21] I. Brihuega, O. Custance, and J. M. Gomez-Rodriguez, Phys. Rev. B **70**, 165410 (2004).
[22] L. Pizzagalli and A. Baratoff, Phys. Rev. B **68**, 115427 (2003).
[23] R. Perez, M. C. Payne, I. Stich, and K. Terakura, Phys. Rev. Lett. **78**, 678 (1997).

[24] S. Hembacher, F. J. Giessibl, and J. Mannhart, Science **305**, 380 (2004).
[25] Y. Sugimoto, T. Namikawa, M. Abe, and S. Morita (unpublished).
[26] H. Uchida, D. Huang, F. Grey, and M. Aono, Phys. Rev. Lett. **70**, 2040 (1993).
[27] B. C. Stipe, M. A. Rezaei, and W. Ho, Phys. Rev. Lett. **79**, 4397 (1997).